A Hybrid Detection Scheme of Architectural Distortion in Mammograms Using Iris Filter and Gabor Filter

Mizuki Yamazaki[1], Atsushi Teramoto[1(✉)], and Hiroshi Fujita[2]

[1] Graduate School of Health Sciences, Fujita Health University, Aichi, Japan
82015309@fujita-hu.ac.jp
[2] Graduate School of Medicine, Gifu University, Gifu, Japan

Abstract. Architectural distortion in mammograms is the most frequently missed finding among breast cancer findings, the improvement of detection accuracy in existing commercial CAD software remains a challenge. In this study, in order to improve the detection accuracy of architectural distortion in mammography, we propose a hybrid automatic detection method that combines with the enhancement method of the concentration of line structure and massive pattern. In the method, the detection of the concentration of the line structure is conducted by the adaptive Gabor filter, and the enhancement of the massive pattern is performed by the iris filter. The concentration index is calculated from these filtered images; the lesion candidate regions are obtained. As for false positive (FP) reduction, 15 shape features are calculated from the candidate regions. Then, they are given to the support vector machine; the candidate regions are classified either as true positive or FP. In the experiment, we compared the results of the proposed method and physician interpretation report using 200 images (63 architectural distortions) from a digital database of screening mammography. Experimental results indicate that our method may be effective to improve the performance of computer aided detection in mammography.

Keywords: Computer-aided diagnosis · Mammography · Architectural distortion

1 Introduction

Breast cancer is the most common cancer in women around the world. Mammography screening has been recommended for breast cancer average-risk women over the age of 45 in the United States [1]. However, because most image data is generated in the image diagnosis, it is feared that the burden on the human reader is too high. Recently, computer-aided diagnosis (CAD) is expected to improve the diagnostic performance by reducing the burden on the human reader and preventing the oversight of lesions [2]. CAD for mammography has been used practically. Among the representative findings of breast cancer, it has reported that microcalcification and mass have detection accuracies of more than 90 %, whereas the detection accuracy of architectural distortion is low, approximately 60–80 % [3]. In order to improve the detection accuracy of architectural distortion, many studies have been conducted: Ichikawa et al. analyzed the

A. Tingberg et al. (Eds.): IWDM 2016, LNCS 9699, pp. 174–182, 2016.
DOI: 10.1007/978-3-319-41546-8_23

area of distortion in mammary glands using the mean curvature [4], Gou et al. developed the learning detection method by Fractal analysis and support vector machine, and compared their result with the results of neural networks [5]. Rangayyan et al. analyzed the mammary gland structure by using the Gabor filter [6]. In order to solve this problem, we developed a detection method as well that employed the Gabor filter [7]. However, it was difficult to detect distortion inside the highly concentrated mammary glands. Furthermore, the Gabor filter did not detect the distortion in case of plural findings at the same position in mammography.

In this study, we focus on the image feature of architectural distortion. Architectural distortion has been defined as the distortion and retraction of the breast structure [8]. Therefore, it seems that the obtained image characteristics tend to be massive patterns such as mass because the centers of retraction have low density in the image. In addition, both architectural distortion and mass are often observed in the invasive breast cancer in a mammogram. In order to improve the detection accuracy of architectural distortion in mammography, we propose a hybrid automatic detection method that combines with the enhancement method of the concentration of line structure and massive pattern. Further, we tried to improve the detection accuracy by a false positive (FP) reduction technique using the support vector machine (SVM).

2 Methods

Line structure enhancement processing and massive pattern enhancement processing are applied to the mammogram using the proposed method. After the candidate regions obtained from each processing are integrated, 15 shape features are calculated in each region. The shape features are input to SVM, the candidate regions are classified as true positive (TP) or FP. The procedure of the proposed method is described by the flowchart shown Fig. 1.

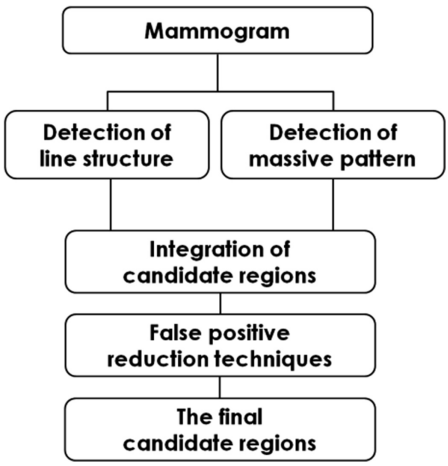

Fig. 1. Flowchart of the proposed method

2.1 Enhancement of Concentration of Line Structure

Normal mammary gland travels radially from the nipple; however, architectural distortion is a disturbance of this structure. In order to analyze the travelling of the mammary gland, the line structure is emphasized and detected using the adaptive Gabor filter that we have developed so far. In addition, architectural distortion often entails local retraction of the mammary gland, which is detected as the region of emphasis on the concentration of line structure. The processing procedure is described below.

(1) **Preprocessing**

By applying automatic binarization using the triangle method [9] and labeling to the original mammogram, unnecessary markers and noise are extracted from the breast region. The triangle method is for automatically calculating the threshold value using the density distribution curve $h(x)$ (x: density) that is obtained by density histogram. In the density distribution curve $h(x)$, the point where the end part of the low density side (the position of $h(x) > 0$) and the point where $h(x)$ is maximized are connected by a straight line. A perpendicular line is taken down to $h(x)$ from each position on the straight line. The position of the perpendicular line that maximizes the distance from both of the intersection until the straight line is searched. The intersection of the obtained perpendicular and $h(x)$ is found, and the corresponding value of the density x becomes threshold value.

(2) **Detection of mammary gland**

The mammary gland is detected by applying an adaptive Gabor filter. The Gabor filter is applied to detect the intensity and the direction of local line structure in the image [10, 11]. The operation expressions of the Gabor filter are shown in Eqs. (1)–(4).

$$g_\theta(x,y) = \exp\left(-\frac{x'^2+\gamma^2 y'^2}{2\sigma^2}\right)\cos\left(2\pi\frac{x'}{\lambda}\right) \tag{1}$$

$$h_\theta(x,y) = f(x,y) \otimes g_\theta(x,y) \tag{2}$$

$$I(x,y) = \max_\theta[h_\theta(x,y)] \tag{3}$$

$$A(x,y) = \operatorname{argmax}_\theta[h_\theta(x,y)] \tag{4}$$

In Eq. (1), the Gabor filter function has an anisotropic shape as shown in Fig. 2. σ is the standard deviation of the Gauss function, which is the parameter that determines the length of the long axis direction. γ represents the spatial aspect ratio of the Gabor function. λ is the wavelength; it is the parameter that adjusts the width of the short axis direction of the filter function. Further, we decide $x' = x\cos\theta + y\sin\theta$ and $y' = -x\sin\theta + y\cos\theta$, because the filter function $g_\theta(x, y)$ is rotated by an angle θ in the x-y plane.

As shown in Eq. (2), the Gabor filter performs a convolution of the original image $f(x, y)$ and the Gabor function $g_\theta(x, y)$ while θ is changed. The angle θ for which

$h_\theta(x, y)$ becomes maximum is calculated ($=\theta_{max}$). The angle θ_{max} becomes $A(x, y)$, $h_\theta(x, y)$ that is calculated using θ_{max} becomes $I(x, y)$. In Eqs. (3) and (4), the intensity output image $I(x, y)$ and the angle output image $A(x, y)$ are shown.

Further, mammary gland detection accuracy using the Gabor filter is significantly affected by the parameters of the Gabor function; therefore, it is not possible to set the parameters that detect all mammary gland patterns. Therefore, adaptive Gabor filter has plural Gabor filters that have different parameter sets, and the optimal filter (best fit filter) is selected for each pixel. This allows improvement in detection accuracy of line patterns compared to a single Gabor filter.

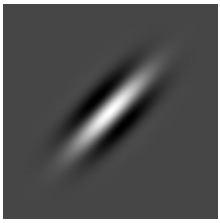

Fig. 2. Gabor filter function (σ = 4.30, γ = 0.45, λ = 13.0)

(3) **Enhancement of the pattern of line concentration**

To detect the concentration of the mammary gland structure, the primary mammary gland is detected by *I(x, y)* and *A(x, y)*. Concentration of the mammary glands caused by retraction and spicula is detected using the concentration index [12].

(4) **Extraction of candidate regions**

The automatic binarization process is applied to the concentration index image. The number of candidate regions and pixel summation are changed by changing the binarization threshold. While changing the threshold for binarization, the number of candidate regions are counted. To increase the detection accuracy, the binarization is performed by the threshold value for which the largest number of candidate regions are detected, and the initial candidate regions of architectural distortion are obtained.

2.2 Enhancement of Massive Pattern

Regarding the detection of a massive pattern in a mammogram, the enhancement of the massive pattern and thresholding are conducted as follows. In a similar manner to the detection of concentration of line structure, processing is applied only to the breast area obtained in Sect. 2.1.

(1) **Enhancement of massive pattern**

The mass of breast cancer has massive structure, because there is the feature that the density in the image decreases toward the center from the edge of the mass, the gradient vector of changing density of each pixel in the mass is concentrated toward its center.

Architectural distortion is the finding of breast cancer that has distortion and retraction of the breast structure. Therefore, it seems that it has the massive pattern like mass and the gradient vector concentrates toward the center. In order to calculate the concentration index of the gradient vector, the iris filter [13] is used in this study. By using the iris filter, the concentration index is calculated from the angle information of the gradient vector of each pixel. As shown in Fig. 3, the pixels on the radial line of the N that are extended in any direction from the interest pixel are used. In each the radiation of the N, the range that maximizes the average of the cosine value of the angle formed by the direction from each pixel to the center point and the gradient vector at each pixel is searched. The concentration index c_j in that direction is the average of the cosine value in obtained range, as shown Eq. (5). The $\cos\theta_{ij}$ is the centrality evaluation value on the j-th of radiation and in radius vector i. R is the outer diameter of the filter and the r is the inner diameter when the pixel of interest is in the center. The iris filter output $C(x, y)$ is the average of the c_j obtained in all directions, as shown Eq. (6).

$$c_j = \max\left\{\sum_{i=0}^{n} \cos\theta_{ij}/i\right\}, R \leq n < r \tag{5}$$

$$C(x,y) = \frac{1}{N}\sum_{j=0}^{N} c_j \tag{6}$$

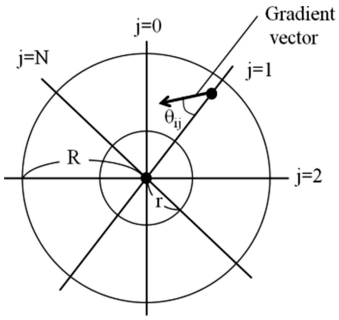

Fig. 3. Conceptual diagram of the iris filter

(2) **Extraction of candidate regions**

The concentration index image obtained from the iris filter is binarized; candidate regions of massive pattern enhancement process are extracted.

(3) **Integration and FP reduction**

The integrated candidate regions are obtained by taking the logical sum of the obtained candidate regions from each method.

Then, for FP reduction, shape features that reflect characteristics of architectural distortion and normal mammary gland structure are calculated for each candidate region. Shape features have 15 types: circularity, perimeter, average in the candidate region, contrast of the margin and center, etc. The calculated shape features are given to the SVM, which classifies FP and TP. The candidate regions that are not deleted as FPs are regarded as the final candidate regions.

3 Experiments

3.1 The Evaluation

In order to confirm the effectiveness of the proposed method, we conducted an evaluation using clinical images. We used 50 cases and 200 images provided by the Digital Database for Screening Mammography (DDSM) that has been published in the United States. This includes 20 normal cases and 30 abnormal cases with architectural distortion. The physician's report that has been attached to the data reveals that the 200 images have 63 architectural distortions. Further, there have been included cases that have architectural distortion only as well as cases with architectural distortion in mass. We evaluated the true-positive rate (TPR) of architectural distortion and FP in images, using physician's report and detection result. In addition, the previous method was applied in the same images, and we compared with TPR and FPs in the previous method and the proposed method. Furthermore, detection accuracy by performing FP reduction was also evaluated.

3.2 Results

In the initial detection without FP reduction, 54 architectural distortions were detected using by the proposed method, TPR was 85.7 %, and the FPs per image was 4.83. An example of a processing result is shown in Fig. 4. The examples of detected and undetected architectural distortion are shown in Figs. 5 and 6, respectively.

4 Discussion

From the result of evaluation by using clinical images, TPR of the initial detection by the proposed method was 85.7 %. That of our previous method was 82.45 %; The detection accuracy was improved over the previous method. The proposed method is added to the massive pattern enhancement process of the previous method, which could detect clearly massive shadow as mass. Moreover, it was possible to detect the massive pattern that secondarily occurred in the spicula and the around of retraction of the mammary gland structure. Therefore, it was shown from the evaluation result that the proposed method was effective to detect architectural distortion accompanied by mass. It is possible that the architectural distortion that could not be detected by the proposed method was excluded from the candidate regions by binarization, because the output

value of each filter became small. Furthermore, due to the shape features, it is possible that the candidate regions are considered FPs by FP reduction processing.

After applying the FP reduction, FPs per image was 3.41 with the same TPR as initial detection. Using FP reduction method, 30 % of FPs were reduced; It became clear that the number of FP could be reduced by using SVM. Many FP regions that were not completely removed existed in locally high density in the image and high concentration of mammary glands in the entire breast. In the future, the shape features that focus on image characteristics will be calculated, and it will be necessary to consider more detailed FP reduction techniques.

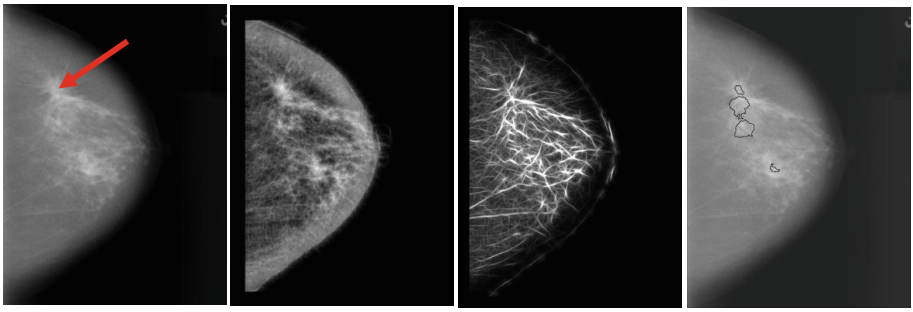

Fig. 4. Example of automated detection using clinical image. Arrow indicates the architectural distortion. (a) Original image, (b) Iris filtered image, (c) Intensity image by adaptive Gabor filter, (d) Detection result

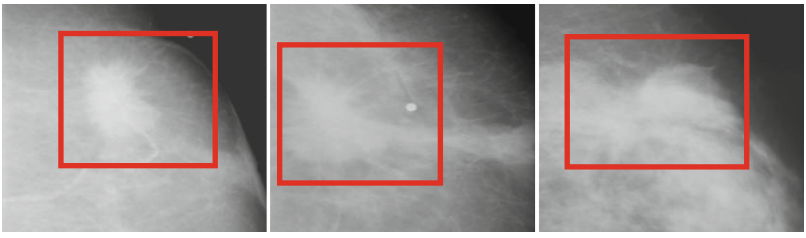

Fig. 5. Examples of detected architectural distortion

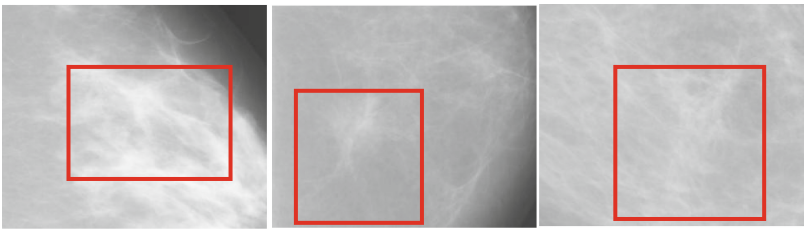

Fig. 6. Examples of undetected architectural distortion

5 Conclusion

In this study, in order to improve the detection accuracy of architectural distortion in mammography, we proposed a hybrid automatic detection method that combined with the enhancement method of the concentration of line structure and massive pattern. In the experiment using 50 cases (200 images) mammography, out of 63 architectural distortions, 54 regions were detected, and the TPR was 85.7 % It was possible to detect architectural distortion accompanied with mass and the massive pattern that secondarily occurred. Furthermore, at that time, FPs without FP reduction was 4.83 per image. However, FPs with FP reduction by using SVM was 3.41 per image. From this result, it is clear that FP reduction with SVM using the shape features is an effective technique. As future challenges, it will be necessary to further improve the detection accuracy and consider more detailed FP reduction methods.

Acknowledgment. This research was supported in part by a Grant-in-Aid for Scientific Research on Innovative Areas (#26108005), MEXT, Japan.

References

1. Oeffinger, K.C., et al.: Breast Cancer screening for women at average risk 2015 guideline update from the American Cancer Society. JAMA **314**(15), 1599–1614 (2015)
2. Fujita, H.: Present status of mammography CAD system. Med. Imaging Technol. **20**(1), 27–33 (2003)
3. Hatanaka, Y., Matdubara, T., Hara, T., et al.: A comparison between physicians' interpretation and a CAD system's Cancer detection by using a Mammogram database in a physicians' self-learning course. Radiol. Phys. Tech. **58**(3), 375–382 (2002). In Japanese
4. Ichikawa, T., Matsubara, T., Fujita, H., et al.: An automated extraction method for region of architectural distortion with concentration of mammary gland on mammograms. IEICE Trans. D-II **87**(1), 348–352 (2004)
5. Guo, Q., Shao, J., Ruiz, V.: Investigation of support vector machine for the detection of architectural distortion in mammographic images. Institute of Physics Publishing **15**, 88–94 (2005)
6. Rangayyan, R.M., Ayres, F.J.: Gabor filter and phase portraits for the detection of architectural distortion in mammograms. Med. Bio. Eng. Comput. **44**, 883–894 (2006)
7. Yoshikawa, R., Teramoto, A., Matsubara, T., Fujita, H.: Detection of architectural distortion and analysis of mammary gland structure in mammograms using multiple Gabor filters. Med. Imaging Technol. **30**(5), 287–292 (2012). In Japanese
8. The Japan Radiological Society and The Japan Society of Radiological Technology: Mammography Guidelines, 3rd edn. Igaku-Shoin Ltd., Tokyo (2014). In Japan
9. Zack, G.W., Rogers, W.E., Latt, S.A.: Automatic measurement of sister chromatid exchange frequency. J. Histochem. Cytochem. **25**(7), 741–753 (1977)
10. Grigorescu, S.E., Petkov, N., Kruizinga, P.: Comparison of texture feature based on Gabor filter. IEEE Trans. Image Process. **11**(10), 1160–1167 (2002)

11. Yoshikawa, R., Teramoto, A., Matsubara, T., Fujita, H.: Automated detection of architectural distortion using improved adaptive Gabor filter. In: Fujita, H., Hara, T., Muramatsu, C. (eds.) IWDM 2014. LNCS, vol. 8539, pp. 606–611. Springer, Heidelberg (2014)
12. Megata, Y., Oza, K., et al.: Features of local concentration patterns in line figures and their applications. IEICE Trans. D-II **77**, 1178–1179 (1994). In Japanese
13. Takeo, H., Shimura, K., Kobatake, H., Nawano, S.: Computer-aided diagnosis in CR mammography. Fujifilm Res. Dev. **43**, 47–54 (1997). In Japanese